Theoretical study of Mn *K*-edge in $La_{1-x}Ca_xMnO_3$

Ignatov A. Yu.,[a,c*] Khalid S.,[b] Sujoy R.[c] and Ali N.[c]

[a] *Physics Department, NJIT, Newark, NJ 07102, USA,* [b] *National Synchrotron Light Source, BNL, Upton, NY 11973, USA,* [c] *Physics Department, SIUC, Carbondale, IL 62901, USA.*
Email:alexander.ignatov@njit.edu

Effects of (i) local magnetic ordering, (ii) lattice distortions, and (iii) Mn 3*d* - O 2*p* hybridization on the shape of Mn *K*- edge XANES spectra of $La_{1-x}Ca_xMnO_3$ have been evaluated numerically and compared with available experimental data. We calculated the spin-polarized Mn *K*-edge spectra. An energy splitting between spin-up and spin-down XANES of 0.5-1.1 eV contributes to the broadening of the total XANES below $T_N(T_c)$. To simulate lattice polaronic distortions across a MI transition the Mn *K*-edge spectra were calculated twice: assuming *R-3c* (*R*=1.96 Å) and *Pbnm* (R_1=1.91, R_2=1.97, and R_3=2.16 Å) symmetries. Results could qualitatively reproduce the observed energy "shift" across the transition. A pre-edge peak at E~ 6542 eV and feature B_3 at ~6 eV above the main peak were found to be related to the Mn 3*d* - O 2*p* hybridization. The feature B_3 should be assigned to a shake-up transition. The calculated *K*-edge spectrum was obtained as a convolution product of the single-electron XANES and the spectrum of many-body excitations in the Mn-O electronic states in the presence of the *1s* core-hole.

Keywords: spin-polarized XANES, Mn 3*d* - O 2*p* hybridization

1. Introduction

This CMRs perovskites $La_{1-x}A_xMnO_{3+\delta}$ (A= Ca, Ba, Sr) are in the focus of the scientific community, especially due to their interesting electronic, magnetic, and structural properties as well as for their potential technological applications. Mn *K*-edge XANES is a powerful tool in identifying the possible electron configurations of Mn ions and in studying the effects of local magnetic ordering and local structure distortions. A systematic evaluation of the Mn configurations is significant because theoretical modeling of the double exchange (DE) mechanism (Zener, 1951) involves the assumption that xMn^{+3} is converted to xMn^{+4}, with x the level of Ca substitution. The Mn atom does not fluctuate between +3 and +4 but shows an "intermediate oxidation state" (Subías *et al*., 1997). However, the authors give few details as to how one should understand this state, which call for further evaluation. Until very recent publication by Bridges *et al*. (2000) that deals with the pre-edge feature at *E*~6542 eV, *none of Mn K-edge XANES included any theoretical calculations*. Lack of detailed spectroscopic studies limits the microscopic understanding of the Mn 3*d* - O 2*p* hybridization phenomena (Mn valence states) and the relationship between the local distortions and local electronic structure.

In this paper we report the Mn *K*-edge near edge structure (XANES) calculations of the $La_{1-x}Ca_xMnO_3$ colossal magnetoresistance compounds considering three pair correlations, according to three fundamental degrees of freedom governing the unusual electronic properties of manganites, namely: the electronic structure of the unoccupied states probed by Mn *K*-edge profile vs.: (i) local atomic distortions; (ii) local magnetic ordering; and (iii) charge-transfer nature of the Mn-O bonds.

2. Experimental

Powder samples of $La_{1-x}Ca_xMnO_3$ (x= 0, 0.3, 1) were prepared by the standard solid-state reaction of La_3O_2, MnO_2, and $CaCO_3$ with several grindings and firings in air at temperatures up to 1480° C as prescribed in the original publications. X-ray powder diffraction measurements affirmed that the samples were a single phase. Diffraction patterns of all samples, except for $LaMnO_{3.15}$, were refined in terms of the orthorhombic space group *Pbnm*, consistent with previous diffraction measurements. $LaMnO_{3.15}$ belongs to the rhombohedral *R-3c* space group. Magnetic properties were investigated using Quantum Design SQUID magnetometer. Metallic sample with x= 0.3, shows ferromagnetic to paramagnetic phase transitions on warming at ~230 K.

Mn K-edge XANES measurements were performed on the beamline X-19a at the Brookhaven National Synchrotron Light Source using a double crystal Si(111) monochromator. The energy scale was calibrated assigning *E*=6539.1 eV to the first inflection point of the pure Mn foil. In order to suppress the remaining La *L* edge oscillations the XAS spectra were collected in the fluorescent yield mode using a 13-element Ge detector with energy resolution ~180 eV. From three to six scans per sample were taken to improve the signal-to-noise ratio. All experimental spectra were collected between 30 and 300 K.

3. Local structure

To study the lattice effect in the manganites we have performed single electron calculations of the Mn *K*- edge in $La_{1-x}Ca_xMnO_3$ (x= 0, 0.3). The spectra were calculated in the real space using the formalism of multiple scattering (MS) of the photoelectron in a cluster of finite size. Mn *K*-edge absorption was treated in the dipole approximation implying an electronic transition from the Mn 1s core level to the unoccupied state above the Fermi level projected on the Mn site and having 4*p* symmetry.

Calculated Mn *K*-edge XANES of $LaMnO_3$ is plotted in Fig. 1 along with the experimental data (background subtracted). Both spectra were normalized to 1.0 at ~100 eV above the absorption threshold. As it is clearly seen from the figure, positions of most features labelled A_i, B_i, C_i, and D_i can be reasonably explained in terms of single-electron MS calculations. However, the intensity of the pre-edge peak at 6542 eV is low and the B_3 feature that is approximately 6 eV above the main peak is missed.

Fig 2(a) shows two experimental Mn *K*-edge spectra of $La_{0.7}Ca_{0.3}MnO_3$ taken below and above the MI transition temperature. We find an energy shift ~0.2eV while the temperature increases from 30 to 260K, that is indicative of changes in the electronic and atomic structure. Here we will restrict ourselves to only structural distortions, performing single-electron MS calculations. In order to simulate polaronic distortions across the MI transition the XANES spectra were calculated twice: (i) assuming *R-3c* symmetry of the cluster with a single Mn-O bond (*R*=1.96 Å), and (ii) using *Pbnm* symmetry of the cluster with three different Mn-O bonds (R_1=1.91, R_2=1.97, R_3=2.16Å). It should be mentioned that a recent EXAFS study of $La_{0.75}Ca_{0.25}MnO_3$ (Lanzara *et al*., 1998) gave supporting evidence for polaronic distortions in the metallic phase. The oxygen atomic distribution with respect to the Mn site was found to be a two-peak function: four short (~1.92Å) and two long (~2.01Å) bonds.

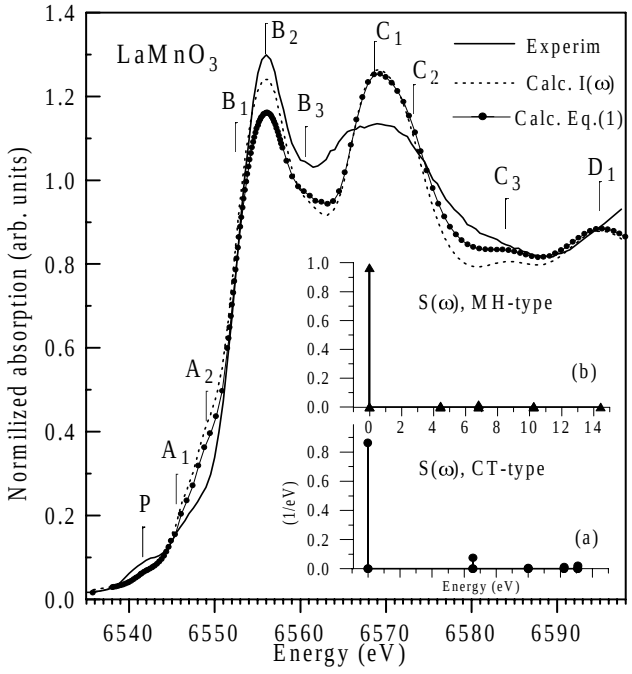

Figure 1
A comparison of the Mn *K*-edges of $LaMnO_3$. The solid line corresponds to the experimental spectrum at 300 K; dashed line shows the result of the single-electron MS calculations for the 87-atom cluster; thin solid line with closed circles represents the convolution of the single-electron spectrum with the CT- excitation spectrum shown in the insert (a). Applying Eq. (1) gives rise to the shake-up peak B_3, lowers the intensities of the A_1 and A_2 features and improves the agreement in the extended area E≥6575 eV.

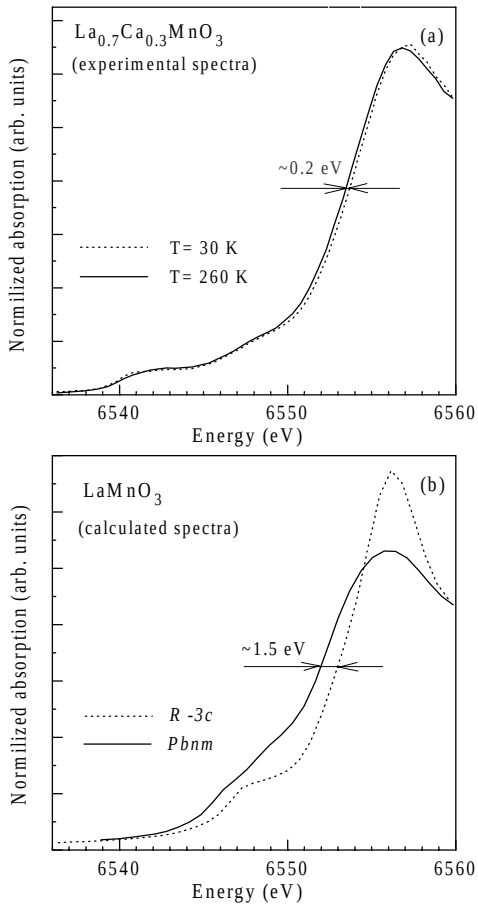

Figure 2
(a) Normalized Mn *K*-edges of $La_{0.7}Ca_{0.3}MnO_3$ measured at 30 K (dashed line) and 260 K (solid line). (b) Calculated XANES spectra showing the profound effect of local atomic distortions on the shape of the edge: fully developed (removed) distortions are simulated assuming orthorhombic (rhombohedral) structure.

In the insulator regime the system shows a three-peak distribution that has been interpreted as two different MnO_6 octahedra. Nevertheless, we still lack information about how to match these different octahedra in the real space that does not allow us to build up the large cluster for the MS calculations. Consequently, the approximation chosen for cluster construction is not unique, though it involves qualitative changes in the Mn-O bond length distribution. As revealed in Fig. 2(b) the shape of the Mn *K*-edge XANES depends dramatically on the local oxygen atomic distribution. In the "metallic" phase the edge is sharper than in the "insulator" phase. The still larger changes in the calculated spectrum could due to the approximations made in cluster construction: The effect of removing Mn-O distortions upon cooling seemed to be overestimated (from three to one Mn-O distance in our simulations vs. from three to two distances suggested by Lanzara *et al* (1998)). In addition, a structure of $LaMnO_3$ was used to model the XANES of the x= 0.3 sample.

To summarize, our MS calculations could qualitatively reproduce the observed energy shift, which, would be better interpreted as spectral intensity redistribution upon the distortions rather than the rigid energy shift.

4. Magnetic ordering

Ensured that we can describe the major source of magnetic ordering in CMR compounds reasonably well (Ignatov & Khalid) we have performed spin-polarized Mn *K*- edge calculations for x= 0, 0.3, and 1. There are energy shifts between the spin-up and spin-down spectra for all compounds originating from the spin-dependence scattering of the photoelectron in the final states. Spin-up and spin-down photoelectrons feel different scattering potentials because of different Mn 3*d* spin densities. This leads to some difference in the partial phase shifts with the largest impact on resonant *d*- type scattering. The atomic-like $1s \rightarrow 4p$ dipole matrix element is also spin-dependent. The spin-up atomic cross section is shifted towards the low energy providing a larger relative intensity for low energy peaks in the spin- up XANES. The resulting spectra are shown in Fig. 3.

Direct experimental observation of spin-up and spin-down XANES of CMRs is a very sophisticated experiment that has not been reported yet. However, the splitting for spin-up and spin-down XANES spectra will contributes to the broadening of the total (conventional) spectrum. The conventional Mn *K*-edge spectrum is given by a sum of spin-up and spin-down spectra: $XANES(E) = 0.5(XANES_{\uparrow}(E) + XANES_{\downarrow}(E))$. The energy shift at the half-height of the edge reaches the maximum of 1.1 eV in the "metallic" x=0.3 sample. The shifts of ~0.9 and ~0.5 eV are found in $LaMnO_3$ and $CaMnO_3$ roughly following the magnitude of the local magnetic moments on the Mn sites as observed by neutron-diffraction measurements (Wollan & Koehler, 1955). Apparently, the "metallic" ($0.2<x<0.4$) samples, the resultant XANES spectrum should become sharper when crossing T_c on warming. However this effect is overshadowed by dramatic increase of local atomic distortions above T_c bringing large spectral redistribution as we have discussed in the previous section.

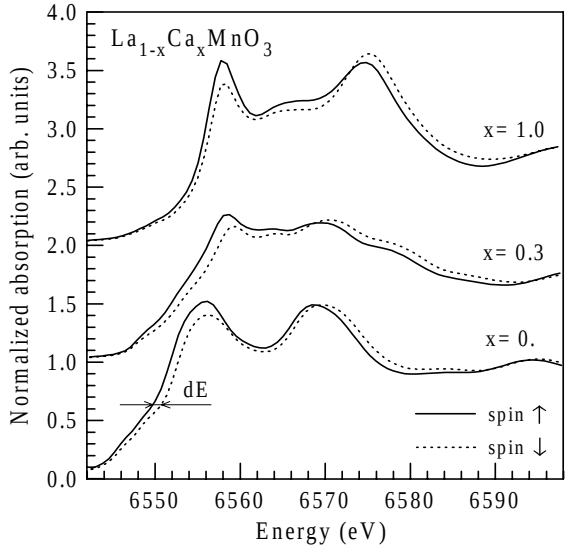

Figure 3
The theoretical spin-polarized Mn *K*-edges of *x*= 0, 0.3, 1 after broadening. Spectra of the *x*= 0.3 and *x*= 1 samples are offset by 1 and 2 for clarity.

5. Mn 3*d* - O 2*p* hybridization

One important aspect of CMR perovskites that, however, is not sufficiently discussed in previous Mn *K*-edge XANES researches, is the essentially covalent character of the Mn-O bonds, as in the Cu based HTSCs. O *K*-edge measurements show that Ca doping introduce the holes and these holes are primarily on the O *2p* rather than on the Mn *3d* orbitals (Park *et al*., 1996; Pellegrin *et al*., 1997). How do the holes affect the shape of the Mn *K*-edge? We can point out two features of the absorption edge shown in Fig. 1 that are related to the Mn 3*d* - O 2*p* hybridization: (i) a pre-edge peak at *E*~ 6542 eV and (ii) the feature B_3 that is ~6 eV above the absorption maximum. The interpretation of the pre-edge is not straight forward (Bridges *et al*., 2000), it shall not be discussed in this brief paper. Instead we will focus on the B_3 feature.

Calculated *K*-edge XANES spectrum can be obtained as a convolution product of the single-electron transition from the *1s* core-level to the unoccupied electronics states, $I(\omega)$, and the spectrum of many-body excitations in the electronic states in the presence of the *1s* core-hole, $S(\varepsilon)$:

$$\sigma(\omega) = \int S(\omega) I(\omega - \varepsilon) d\varepsilon \qquad (1)$$

$$S(\omega) = \sum \left| \left\langle \Psi_f^i \middle| \Psi_0 \right\rangle \right|^2 \delta(\omega - E_i + E_0) \qquad (2)$$

where Ψ_0 is the ground state with energy E_0 and Ψ_f is the *i*-th excited state with energy E_i referred to Hamiltonians in the initial H_0 and final states H_f respectively. In the case of CMR compounds, the Hamiltonian referred to the wavefunctions in Eq. 2 is not well established yet. It seems to have to be a combination of the Anderson-Hasegawa (1955) and Peierls-Hubbard Hamiltonians (see, for example, Ignatov, 1999). Since in this section we explore the role of the Mn 3*d* - O 2*p* hybridization, simplified calculations for the low-spin system ignoring the charge-lattice and spin-lattice couplings are presented.

Charge-transfer (CT) and Mott-Hubbard (MH) regimes implying, respectively, O 2*p* and Mn 3*d* character of the doped states have been considered. Only three parameters of the 2D Hubbard Hamiltonian were used: Δ= 4.5, U_d= 7.8, and t_{pd}=5.4 eV for the CT (Saitoh *et al*., 1995) and Δ= 5, U_d= 4, and t_{pd}=6.6 eV (Chainani *et al*., 1993) for the MH-type. The Mn 1s-3*d* Coulomb repulsion, Q , was taken equal to U_d. Inspection of the CT-excitation spectrum shown in the insert (a) of Fig. 1 reveals that approximately 7% of total spectral weight stands at 6.2 eV *above* the major peak. According to Eq. 1 this gives rise to the so-called *shake-up* transition: peak B_3 appears in the calculated spectrum shown by solid line with dots. In contrast, the MH-regime has very low intensity of the satellite peaks, clearly insufficient to provide a reasonable magnitude for the B_3 feature. Thus, our theoretical analysis of Mn *K*-edge of $LaMnO_3$ supports O 2*p* character of doped states.

6. Conclusion

We have considered *separately* the effects of magnetic ordering, lattice distortions, and Mn 3*d* - O 2*p* hybridization upon the shape of the Mn *K*-edge in $La_{1-x}Ca_xMnO_3$ (*x*= 0, 0.3, 1). Mn *K*- edge is dominated by dipole $1s \rightarrow 4p$ transition. Main features at the absorption edge can be qualitatively reproduced in terms of single-electron MS calculations for the large cluster of atoms. For the first time we have calculated spin-polarized XANES spectra. We anticipate experimental Mn *K*-edge SPXANES will be reported soon that would open a road for the direct comparison of calculated and measured spectra. A small feature, B_3, standing approximately 6 eV above the main absorption peak is beyond single-electron calculations including the spin-polarized ones. Experimental observation of the shake-up peak and Hamiltonian's parameters used in the calculations both imply that $LaMnO_3$ should be viewed as a charge-transfer-type insulator with a *substantial O 2p component in the ground state*. This agrees with results by Ju *et al.* (1997) implying that O 2*p* holes contribute significantly to the conduction mechanism, including the magnetoresistance. Our findings support recent theory of Alexandrov & Bratkovsky (1999) rather than the "intermediate" Mn valence (Subías *et al.*, 1997) and conventional DE mechanism (Zener, 1951) both implying 3*d* character of doped states. We argue (Ignatov & Khalid) that the Mn valence may be understood as a mixture of the charge-transfer many-body electronic configurations: $\alpha|3d^5> + \beta|3d^4> + \gamma|3d^5L> + \delta|3d^6L^2> + \varepsilon|3d^3> + \zeta|3d^4L> + \eta|3d^5L^2> + \theta|3d^4L^2>+ \ldots$ coupled with spin and lattice degrees of freedom.

This work was supported in part by the Consortium for Advanced Radiation Source, University of Chicago. Data acquisition was done at the NSLS supported by the DOE under contract number DE-AC02-98CH10886.

References

Alexandrov, A. S. & Bratkovsky, A. M. (1999). *Phys. Rev. Lett*. **81**, 141-144.
Anderson, P. W. & H. Hasegawa, H. (1955). *Phys. Rev*. **100**, 675-681.
Bridges, F., Booth, C. H., Kwei, G. H., Neumeier, J. J. & Sawatzky, G. A. (2000). *Phys. Rev*. B **61**, R9237-9240.
Chainani, A., Mathew, M., & Sarama, D. D. (1993). *Phys. Rev*. B **47**, 15397-15403.
Ignatov, A.Yu. (1999). *J. Synchrotron Rad*. **6**, 532-534.
Ignatov, A.Yu. & Khalid, S. *Phys. Rev* B (submitted).
Ju, H. L., Sohn, H. -C., & Krishnan, K. M. (1997). *Phys. Rev. Lett*. **79**, 3230-3233.
Lanzara, A., Saini, N. L., Brunelli, M., Natali, F., Bianconi, A., Radaelli, P.G. & Cheong, S.-W. (1998). *Phys. Rev. Lett*. **81**, 878-881.
Saitoh, T., *et al*. (1995). *Phys. Rev.* B **61**, 13942-13951.
Subías, G., García, J., Proietti, M. G. & Blasco, J. (1997). *Phys. Rev. B* **56**, 8183-8191.
Park, J.-H. *et al*. (1996). *Phys. Rev. Lett*. **81**, 4215-4218.
Pellegrin, E. *et al*. (1997). *J. Phys. IV France* **7**, C2-405-408.
Wollan, E. O. & Koehler, W. C. (1955). Phys. Rev. **100**, 545.
Zener, C. (1951). *Phys. Rev*. **82**, 403-405.